Arch. Metall. Mater. **65** (2020), 1, 103-108

DOI: 10.24425/amm.2019.131102

M. CIESLIK[1*], K. DAROWICKI[1]

# INTERGRANULAR CORROSION DETECTION USING ELECTROMAGNETIC TRANSDUCERS FOR ULTRASONIC TESTING

The aim of this paper is to create a research methodology that allows a quick analysis of the structural state of high alloy austenitic steels using non-destructive ultrasonic tests, in contrast to destructive standard methods. Electromagnetic acoustic transducers (EMAT) are used to generate and receive the ultrasonic wave and detect the microstructural changes caused by sample sensitization in elevated temperature, even after 0.5 h in high temperature exposition. Different acoustic response for reference sample and sensitized samples were recorded. In this work, changes in share wave amplitude were measured.

*Keywords:* intergranular corrosion, NDT, EMAT, ultrasonic testing

## 1. Introduction

Intergranular corrosion is characterized by the selective destruction of the metal at the grain boundaries. Sensitized steel in contact with an aggressive environment starts to corrode, the more active grain boundaries and adjacent areas are corroded, with the grain surface practically unchanged. It is the result of an unfavourable ratio of a large cathode (grain) to a small anode (grain boundary). Sensitization of high alloyed austenitic steel can occur when it is heated in the temperature range 650-800°C [1]. During heating, carbon and chromium diffuse to the grain boundaries, however, the diffusion rate of smaller carbon atoms is higher than that of chromium atoms. In the structure, the chromium is segregated and chromium carbides $Cr_{23}C_6$ are formed at the grain boundaries. The result of the diffusion of chromium atoms is the depleted content in the grain boundary region. The steel which is sensitizing after heating at 650-800°C is not suitable for welding because the heat affected zone will be sensitized to intergranular corrosion [2,3].

Currently, several methods are used to assess the susceptibility of stainless steel to intergranular corrosion. The electrochemical method is distinguished, in which a sample of 304 or 304L steel is placed in a solution of 0.5M $H_2SO_4$ + 0.01 KSCN and then anodically polarized [4]. Standard methods depend on the conditioning of samples at specific temperatures and solutions at a certain time. The microstructure analysis of the etched samples is performed after the test using metallographic microscopes. However, standard methods are destructive and time-consuming [4,5].

Ultrasonic testing is one of few non-destructive methods to evaluate steel, composite, polymer or concrete materials in material volume. The approach enables localization and determination of internal dimensions, surface and subsurface discontinuities, such as: cracks, blisters, thinning, delamination, inclusions, erosion, etc. [6]. The piezoelectric heads commonly used in ultrasonic tests require continuous coupling of the acoustic head with the examined object. Automated testing is hindered, since the element would have to be kept in constant contact with the coupling agent or immersed in it. The necessity of using coupling agent in metal research results from a large difference in acoustic impedance between air and metal [6,7]. The acoustic impedance of materials depends on the density of the medium and on the wave propagation rate in this medium [7]. For air, the value of acoustic impedance is $0.0004 \cdot 10^6$ kg$\cdot$m$^{-2}\cdot$s$^{-1}$, and for steel $46 \cdot 10^6$ kg$\cdot$m$^{-2}\cdot$s$^{-1}$. For such values, the steel/air interface passes only 0.6% of the wave energy. The use of water as a coupling agent with an acoustic impedance of $1.5 \cdot 10^6$ kg$\cdot$m$^{-2}\cdot$s$^{-1}$ significantly improves the situation, since 35% of the wave energy penetrates the investigated sample [8].

Electromagnetic acoustic transducers (EMAT) are used for non-contact generation and acquisition of ultrasonic waves, but are limited to conductive materials. The main components

[1] GDANSK UNIVERSITY OF TECHNOLOGY, FACULTY OF CHEMISTRY, DEPARTMENT OF ELECTROCHEMISTRY, CORROSION AND MATERIALS ENGINEERING, 11/12 NARUTOWICZA STR., 80-233 GDANSK, POLAND

* Corresponding author: matciesl2@student.pg.edu.pl

of the EMAT transducer head are the excitation coil and the permanent magnet or electromagnet [6,9]. The coil is supplied with alternating current at frequencies ranging from 100 kHz to 6 MHz. The electromagnetic field acting on the coil induces eddy currents in the surface layer of the tested object. The flow of current in the material in a permanent magnetic field is the source of the Lorentz's force. The Lorentz force causes vibrations of particles in the surface layer of the material and its cyclical deformations. The frequency of material vibrations is consistent with the frequency of the current with which the coil is excited. The EMAT transmitter operating scheme is presented in Fig. 1. The transducer receives the acoustic response in inversely to generated signal. This means that the mechanical vibrations of the material in a constant magnetic field causes the generation of alternating currents that subsequently generate eddy currents in the transducer [9]. In the case of EMAT heads the Snell's law doesn't apply, and the probe angle doesn't affect the direction of wave propagation [10].

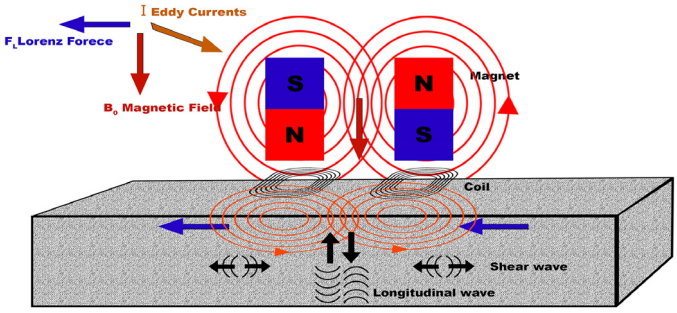


Fig. 1. The scheme of ultrasonic wave generation in tested material using EMAT head

The aim of this paper is to create a research methodology that allows a quick analysis of the structural state of high alloy austenitic steels using non-destructive ultrasonic tests, in contrast to destructive standard methods.

## 2. Experimental

The two sets of samples made of AISI 304 stainless steel were prepared. Both sets were cut using a guillotine in a way to not overheat the material. The first set with dimensions 6 mm×20 mm×20 mm (*thickness, length, width*) was used for microscopic tests and the second one, 6 mm×230 mm×130 mm, for ultrasonic testing. The samples were sensitized in a muffle furnace at the temperature of 700°C for 0.5h, 1h, 2h, 4h and 8h for different degree of sample sensitization. After the heat treatment, the samples were cooled in water. Each surface of the first samples set was mechanically polished on abrasive paper: 600, 1200, 2000 and 4000 grit, subsequentially. At the next step, the diamond suspension with grain size 9 µm and 3 µm were used to get the mirror surface of the sample. Finally, the samples were rinsed in demineralized water, degreased in acetone and electrochemically etched in 10% oxalic acid for the 40s.

The micrographs of sensitized samples were taken using metallographic microscope a Nikon Eclipse MA200 (Japan). Furthermore, the morphology was characterized by a S-3400N scanning electron microscope (SEM) (Hitachi, Japan). The microscope is equipped with a tungsten filament. Micrographs were made with back-scattered electron mode (BSE), at accelerating voltage of 20kV. The SEM was expanded with energy dispersive X-ray spectroscopy (EDS) UltraDry (ThermoFisher Scientific, USA) detector for the examination of chromium carbides segregation at the sample surface.

Ultrasonic tests were carried out using an Innerspec PowerBox H (USA) defectoscope. Butterfly type transmitter/receiver coils and permanent magnet were used to generate shear waves. Burst frequency was 1411 kHz, pulse repetition frequency (PRF) 25 Hz, and the wavelength 0.16 inch. Additionally, defectoscope was equipped with signal conditioning box with tuning module L/SE-PC-M-0.160-1250 kH PE-008 Innerscpec. The shear wave velocity was 3207 m/s.

## 3. Measurements concept

It is possible to perform ultrasonic tests, thickness measurements and studies of the crystalline structure of the material using the defectoscope. The equipment enables its use in laboratory and field conditions when in the data acquisition mode. Impulse packets in the frequency range from 100 kHz to 6 MHz allow generation of each type of wave. The transducer used in these tests had two coils: one capable to generate and receive longitudinal waves, the other capable to generate and receive shear waves. The use of two coils allows assessing which of the waveforms generated has the higher possibilities of detecting chromium carbides at the grain boundaries. the values of changes in the velocity of the wave and their attenuation were measured to determine the degree of sensitization of stainless steel. The differences in the wave velocity can be determined from the spectrum of the received signal in the frequency domain, it is calculated from the following formulas [11]:

$$f_n = \frac{nv}{2d} \tag{1}$$

where: $v$ is the phase velocity of the bulk plane, $d$ is the thickness of the plate, $f_n$ is the resonance frequency of the $n$-th order. The time of flight (*ToF*) of the two following back wall echoes could be calculated from the resonant frequency:

$$ToF = \frac{v}{f_n} \tag{2}$$

When the peak-to-peak amplitude in the frequency domain give the resonant frequency of different orders: $f_n, f_{n+1} f_{n+2}, \ldots$, the fundamental resonant frequency can by calculated with:

$$f_l = \frac{v}{2d} \tag{3}$$

The velocity is given when the frequency and the material thickness is known:

$$v = 2df_l \tag{4}$$

The back walls echoes decreases exponentially and it is shown in equation (5):

$$A_{n+1} = A_1 \exp(-2n\alpha_m d) \tag{5}$$

where: $A_1$ and $A_{n+1}$ are echo heights of the following peaks, $\alpha$ is the attenuation coefficient and d is the material thickness.

The losses of ultrasonic amplitude pressure are connected with the material thickness, wave reflection and wave breakdown in the material. These losses are caused by the wave scattering on grain boundaries, small inclusions, material discontinuities, pores, etc. The impact of the lost ultrasonic wave bundle pressure is mirrored by the echoes string reflected for any defects on the defectoscope screen. The attenuation coefficient strongly depends on wave frequency [12]. The wave suppression had an important role in wave propagation if its length is nearly the same as the grain size. The losses caused by the wave suppression and wave scatter summed up and it is shown in the relationship below [13].

$$20\log\frac{p_z}{p_0} = const - 20\log z - 2\alpha_m z \tag{6}$$

where: $p_0$ [Pa] is an acoustic pressure produced by transducer, $p_z$ [Pa] is an acoustic pressure in the ultrasonic bundle at $z$ represents the distance from the transducer, $\alpha_t$ [dB·m$^{-1}$] is an attenuation coefficient.

EMAT transducers are used to measure the attenuation coefficient $\alpha_m$. It consists of material's attenuation ($\alpha$), the diffraction loss ($\alpha_d$) and the eddy current loss ($\alpha_e$).

$$\alpha_m = \alpha + \alpha_d + \alpha_e \tag{7}$$

The eddy current loss occurs for plane waves and it can be calculated by:

$$\alpha_e = \frac{\eta B_0^2}{2\rho} \tag{8}$$

where: $B_0$ [T] is describes applied static magnetic flux density, $\rho$ [kg·m$^{-3}$] is denounces material density, $\eta$ [S·m$^{-1}$] is defines conductivity.

The $\alpha_e$ for common metals can by neglected because its value is about $10^{-3}$ μs$^{-1}$ [9]. The material's attenuation coefficient is a constant value and can be taken from the various literature sources [12,14].The diffraction loss can be eliminated through so-called correction algorithm resonance [9]. The $\alpha_m$ can be calculated from the echo height ratio of the following peaks with the below shown relationship [15]:

$$\alpha_m = \frac{20\log\left(\frac{A_n}{A_{n+1}}\right)}{2d} \tag{9}$$

where: $A_n$ and $A_{n+1}$ are echoes heights of the following peaks, $d$ is the specimen thickness $m$.

The scheme of the ultrasonic sensitization sample measurements using EMAT transducers is shown in Fig. 2.

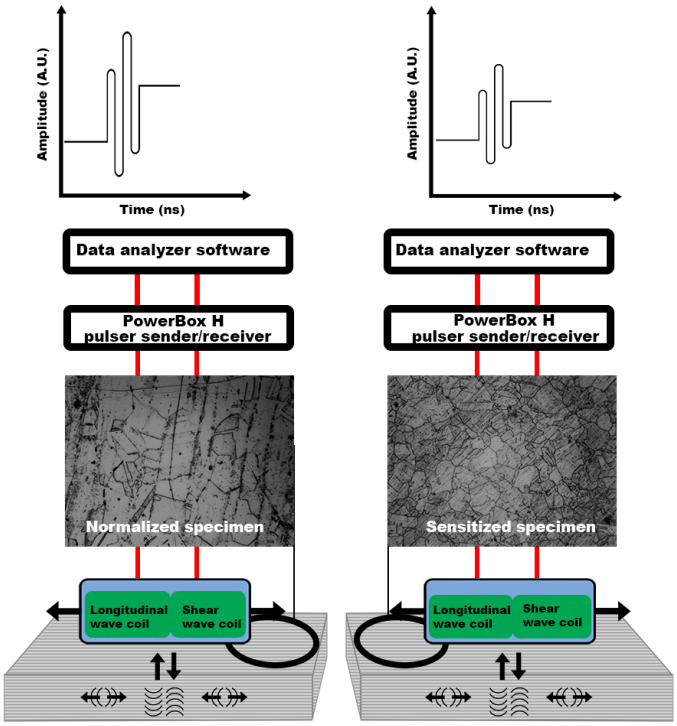


Fig. 2. Schematic representation of the ultrasonic measurement response of normalized and sensitized specimen using EMAT transducers

## 4. Result and discussion

All samples subjected to exposure to elevated temperatures for 0.5h, 1h, 2h, 4h, and 8h undergone sensitization to the intergranular corrosion. This can be confirmed by the presence of chromium carbides at the grain boundaries, visible in Fig. 3. Chromium carbides appear dark on the micrographs (similar as other structural defects), which allows to estimate the ratio of the unchanged material structure (light areas) versus chromium carbides and other surface contaminants such as metal oxides which appears as a result of sample sensitization (dark area).

These results have been presented in Table 1.

TABLE 1

The percentage share of light surfaces to dark areas calculated using a program written in the LabView environment

| No. | Percentage of the light area (%) | Standard deviation (%) |
|---|---|---|
| Reference sample | 80.83 | 2.06 |
| 0.5h sensitized | 68.18 | 1.76 |
| 1h sensitized | 59.65 | 1.92 |
| 2h sensitized | 62.59 | 2.21 |
| 4h sensitized | 63.22 | 2.12 |
| 8h sensitized | 61.61 | 1.05 |

The least modified was the sample exposed to elevated temperatures for the shortest duration of half an hour. The degree

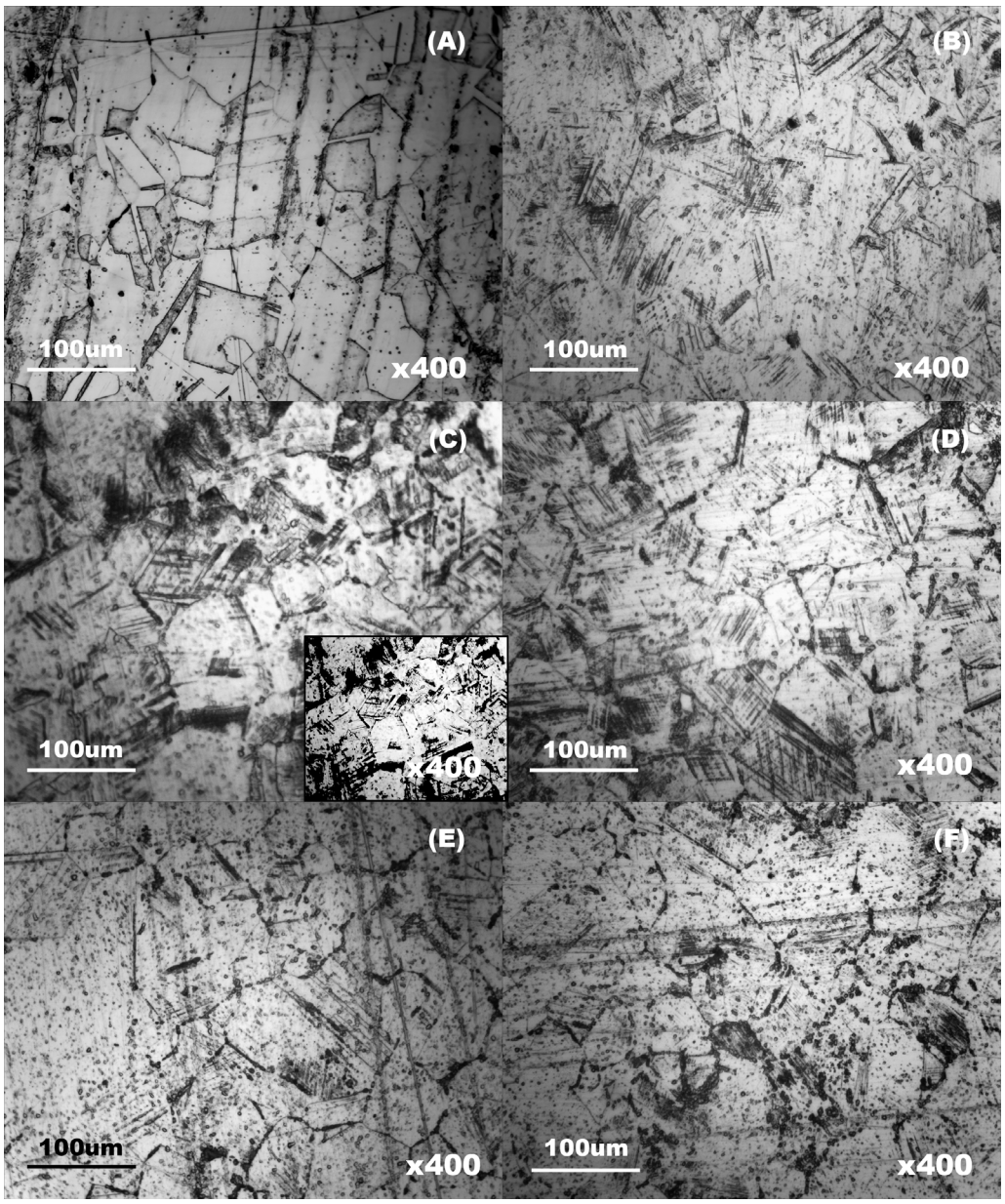


Fig. 3. Metallographic structure for (A) reference sample, (B) 0.5h annealed sample, (C) 1h annealed sample with micrograph after binarization process, (D) 2h annealed sample, (E) 4h annealed sample and (F) 8h annealed sample. In picture (A) the austenite structure is presented. On sensitized sample (picture (B), (C), (D), (E), (F)) on grain boundaries, chromium carbides occur. The scratches marks and the pitting after electrochemical etching are also visible

of sensitization of the other samples remains at a similar level, based on the image binarization procedure.

The morphology of each sample was characterized by SEM in the back-scattered electrons (BSE) mode. The structure of austenite and chromium carbides precipitated at the grain boundary is visible on the sample surface. In addition, pitting is also present on the surface, which could have been caused by the electrochemical etching with oxalic acid. Chemical composition was characterized by EDS technique. There is a significant difference in the local chemical composition. The chromium content is about 44 wt.% at the grain boundaries (Point 1 in Fig. 4), while on the grain surface (Point 2 in Fig. 4) is over two times lower. The chemical composition in each point, for the sample sensitized in the furnace for 1h is shown in Table 2.

TABLE 2

The differences in chemical composition on grain surface and on the grain boundaries

| | Fe wt.% | Cr wt.% | Ni wt.% | Mn wt.% | Si wt.% |
|---|---|---|---|---|---|
| Grain boundaries | 45.8 | 44.7 | 6.3 | 2.5 | 0.7 |
| Grain surface | 66.4 | 18.9 | 12.8 | 0.7 | 1.2 |

The ultrasonic test was performed in Pitch-Catch mode. A transmitter and receiver are used to track the echoes received in the transmission direction. In three out of four sensitized samples, the energy loss caused by the microstructural changes is clearly visible. This loss is naturally connected with chromium carbides precipitation at the grain boundaries. The amplitude changes for all the tested samples were compared to a reference

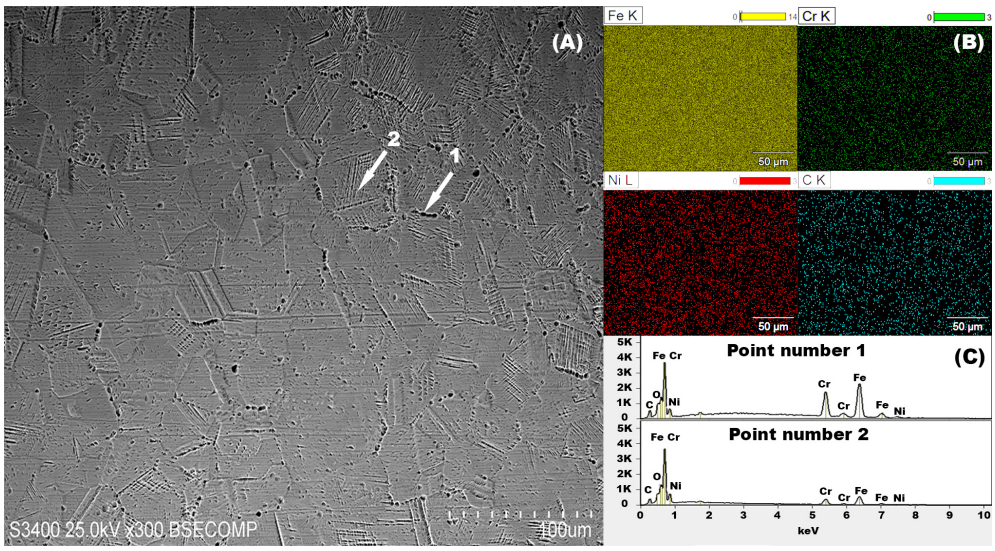


Fig. 4. SEM micrograph of surface morphology for a sample annealed 1h in a muffle furnace made in BSE mode. Point number 1 is located grain boundaries, point number 2 on the grain surface (A). The chemical surface maps (B) the distribution of the elements is uniform. The spectra for each point are showed in (C), the chromium content for point 1 is much bigger than for point 2

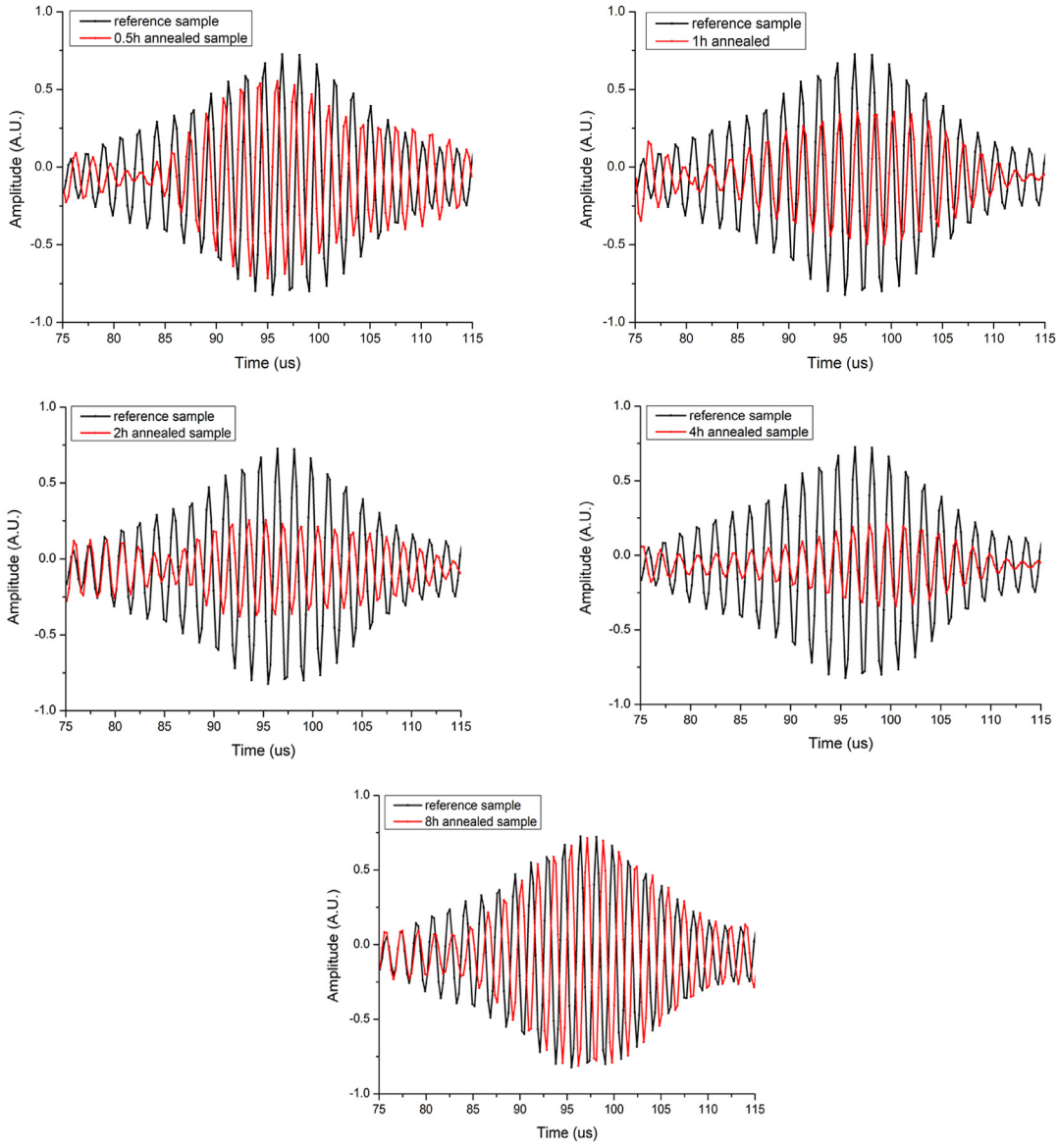


Fig. 5. Different acoustic response for sensitized samples compared to the reference sample

sample amplitude using the second back wall echo in order to avoid interference phenomena caused by the near-field to assess the sensitization of steel [16]. The results are presented in Fig. 5 are the average value obtained on the basis of five measurements in different places of the tested samples. Sample sensitized for the shortest duration show some amplitude difference, yet it is not as evident as in the case of samples sensitized for 1 h, 2 h, 4 h. The wave suppression increased with sensitized time up to 4 h. The ultrasonic spectra for the 8 h sensitized sample are very similar to the reference sample. This can be explained by that a long-time heat treatment is used as one of the post process intergranular corrosion prevention methods [1]. The amplitude differences are shown in Table 3.

TABLE 3

The amplitude differences for sensitized samples compared to the reference sample after the ultrasonic test

| No. | Amplitude differences (A.U.) | Standard deviation (A.U) |
|---|---|---|
| 0.5h sensitized | 0.10 | 0.01 |
| 1h sensitized | 0.11 | 0.02 |
| 2h sensitized | 0.27 | 0.02 |
| 4h sensitized | 0.30 | 0.01 |
| 8h sensitized | 0.01 | 0.03 |

## 5. Conclusion

The conducted research shows that the time of exposure of the sample at high temperature influences the degree of its sensitization. Non-contact ultrasonic testing using electromagnetic acoustic transducers (EMAT) are able to detect structural differences of sensitized samples, even after 0.5 h sensitization time. The amplitude of the shear wave of sensitized samples compared to the reference sample changes with the exposure time at elevated temperature. A different situation occurs for the sample heated for 8 hours. The acoustic response for this sample is practically the same as for the reference sample. As mentioned before, a long heating time could lead to the homogenization of the structure. Direct correlation between ultrasonic method and binarization method is not entirely possible because the whole surface is not examined but only a fragment of a microscopic image. The presented measuring method has potential limitations in relation to the time in which a given sample was sensitized. The authors conduct further research on increasing the scope of applicability of a given measuring method.

## REFERENCES


[1] A.J. Sedriks, O.S. Zaroog, Corrosion of Stainless Steels☆, in: Reference Module in Materials Science and Materials Engineering, Elsevier, 2017. doi:10.1016/B978-0-12-803581-8.02893-9.

[2] D. Talbot, J. Talbot, Corrosion science and technology, CRC Press, Boca Raton, 1998.

[3] J. Baszkiewicz, M. Kamiński, Korozja materiałów, Oficyna Wydawnicza Politechniki Warszawskiej, Warszawa, 2006.

[4] G01 Committee, Test Method for Electrochemical Reactivation (EPR) for Detecting Sensitization of AISI Type 304 and 304L Stainless Steels, ASTM International, n.d. doi:10.1520/G0108-94R04E01.

[5] A01 Committee, Practices for Detecting Susceptibility to Intergranular Attack in Austenitic Stainless Steels, ASTM International, n.d. doi:10.1520/A0262-15.

[6] O. Büyüköztürk, NDTMS, International Union of Laboratories and Experts in Construction Materials, Systems and Structures, eds., Nondestructive testing of materials and structures: proceedings of NDTMS-2011, Istanbul, Turkey, May 15-18, 2011; [International Symposium on Nondestructive Testing of Materials and Structures], Springer, Dordrecht, 2013.

[7] L.E. Kinsler, ed., Fundamentals of acoustics, 4th ed, Wiley, New York, 2000.

[8] J. Szelążek, Tworzywa sztuczne jako ośrodki sprzęgające w ultradźwiękowych badaniach materiałów, TWORZYWA SZTUCZ NE I CHEMIA. (2010).

[9] M. Hirao, H. Ogi, EMATs for Science and Industry: Noncontacting Ultrasonic Measurements, Springer US, Boston, MA, 2003. http://public.eblib.com/choice/publicfullrecord.aspx?p=3086206 (accessed November 28, 2018).

[10] A.K. Wróblewski, Historia fizyki od czasów najdawniejszch do wspólczesności, Wyd. 1., 2. dodruk, Wydawn. Naukowe PWN, Warszawa, 2007.

[11] F. Li, D. Xiang, Y. Qin, R.B. Pond, K. Slusarski, Measurements of degree of sensitization (DoS) in aluminum alloys using EMAT ultrasound, Ultrasonics **51**, 561-570 (2011). doi:10.1016/j.ultras.2010.12.009.

[12] J. Deputat, Badania ultradźwiękowe. Podstawy, Instytut Metalurgii Żelaza im. St. Staszica i Ośrodek Doskonalenia Kard Kierowniczych i Specjalistycznych Ministerstwa Hutnictwa, Gliwice-Chorzów, 1979.

[13] A. Lewińska-Romicka, Badania nieniszczące podstawy defektoskopii, n.d.

[14] J. Deputat, A. Stryk, Badania ultradźwiękowe. Kurs UT1. Materiały szkoleniowe., (1997).

[15] J. Stella, J. Cerezo, E. Rodríguez, Characterization of the sensitization degree in the AISI 304 stainless steel using spectral analysis and conventional ultrasonic techniques, NDT & E International. **42**, 267-274 (2009). doi:10.1016/j.ndteint.2008.11.005.

[16] K. Mirkhani, C. Chaggares, C. Masterson, M. Jastrzebski, T. Dusatko, A. Sinclair, R.J. Shapoorabadi, A. Konrad, M. Papini, Optimal design of EMAT transmitters, NDT & E International. **37**, 181-193 (2004). doi:10.1016/j.ndteint.2003.09.005.